Original Article

JCBFM

Journal of Cerebral Blood Flow & Metabolism
2020, Vol. 40(12) 2475–2490

DOI: 10.1177/0271678X19895245
journals.sagepub.com/home/jcbfm
SAGE

Susceptibility to capillary plugging can predict brain region specific vessel loss with aging

Ben Schager[1] and Craig E Brown[1,2]

Abstract

Vessel loss in the aging brain is commonly reported, yet important questions remain concerning whether there are regional vulnerabilities and what mechanisms could account for these regional differences, if they exist. Here we imaged and quantified vessel length, tortuosity and width in 15 brain regions in young adult and aged mice. Our data indicate that vessel loss was most pronounced in white matter followed by cortical, then subcortical grey matter regions, while some regions (visual cortex, amygdala, thalamus) showed no decline with aging. Regions supplied by the anterior cerebral artery were more vulnerable to loss than those supplied by middle or posterior cerebral arteries. Vessel width and tortuosity generally increased with age but neither reliably predicted regional vessel loss. Since capillaries are naturally prone to plugging and prolonged obstructions often lead to vessel pruning, we hypothesized that regional susceptibilities to plugging could help predict vessel loss. By mapping the distribution of microsphere-induced capillary obstructions, we discovered that regions with a higher density of persistent obstructions were more likely to show vessel loss with aging and vice versa. These findings indicate that age-related vessel loss is region specific and can be explained, at least partially, by regional susceptibilities to capillary plugging.

Keywords

Microcirculation, vascular dementia, white matter, aging, cerebral blood flow, capillary rarefaction

Received 14 August 2019; Revised 28 October 2019; Accepted 19 November 2019

Introduction

Without substantial local energy stores, the brain demands a constant supply of oxygen and nutrients.[1,2] In order to meet this demand the brain is densely supplied with capillaries which are narrow, low-pressure, high surface area vessels that comprise the majority of cerebral vascular length and are always in close proximity (~13–18 μm) to neurons and glia.[3–6] As such, it is not surprising that age and disease-related vascular changes that result in reduced capillary number and perfusion correlate with and contribute to cognitive impairment and dementia, including Alzheimer's Disease and Vascular Dementia.[7–11] Indeed, a recent study revealed a direct link between capillary blood flow and cognition by showing that unplugging cortical capillaries could improve blood flow and memory in a mouse model of Alzheimer's disease.[12]

Although it is well appreciated that capillary networks are important for maintaining brain function with aging, there still exists debate over the extent to which vascular density changes over the lifetime. For example, several rodent studies indicate there is profound vessel loss within a few regions over 1–2 years of age, whereas other studies indicate no change at all.[13–16] Further, to our knowledge no aging study has systematically surveyed vascular changes across a multitude of brain regions. Given long standing evidence that certain brain regions are particularly vulnerable to functional decline with aging, such as white matter tracts, limbic cortex and hippocampus,[17–19] comparing vessel loss

[1]Division of Medical Sciences, University of Victoria, Victoria, BC, Canada
[2]Department of Psychiatry, University of British Columbia, Vancouver, BC, Canada

Corresponding author:
Craig E Brown, Medical Sciences Building, PO Box 1700 STN CSC, University of Victoria, Victoria, BC V8W 2Y2, Canada.
Email: brownc@uvic.ca

across many different regions within the same animals could provide valuable comparative data. Revealing such differences will be useful for future "omic" research that seeks to understand regional diversity in aging processes at a molecular level.[20,21]

Another unresolved issue in the aging literature concerns the mechanisms that account for age-related vessel loss. While this is a multifactorial problem involving the relative balance between vessel rarefaction and perhaps sprouting, it is likely that the capillary's inherent susceptibility to clogging, due to adherent white blood cells or debris circulating in the blood (cholesterol, fibrin), could be an important factor. Recently our group and others demonstrated that a small fraction of cortical capillaries experience short and long-lasting obstructions, even in healthy animals.[22–24] Of note, about ~30% of these persistent obstructions led to vessel pruning with little evidence of compensatory sprouting.[24] Using this information, we were able to approximate vessel loss with aging that closely matched our experimentally derived estimate.[24] However, one major limitation of our previous study was that only one brain region was sampled (primary somatosensory cortex) and therefore it is unknown if there are brain region specific differences in the susceptibility for capillaries to become obstructed, and perhaps experience greater vessel loss with age.

Here, we attempt to reconcile some of these discrepancies in the aging literature by performing a broad survey of vascular changes in length, tortuosity and width in 15 different brain regions, including differences that may arise between different classes of brain matter (white vs. grey; cortical vs. subcortical) or perfusion territory. In order to directly label all patent vessels, we intravenously injected a fluorescent dye in vivo and then developed an automated approach for detecting and analyzing fluorescently labeled vessels in post-mortem tissue sections. Furthermore, to help explain regional differences in vessel loss, we induced capillary obstructions with fluorescent microspheres in adult mice and surveyed capillary obstruction rates in each brain region. Our experiments reveal considerable regional heterogeneity in vessel loss with aging that varies based on tissue class and perfusion territory. Further, we find a significant correlation between a specific brain region's susceptibility to capillary plugging and vessel loss with aging. Collectively, these findings suggest that vascular networks within certain brain regions may be more vulnerable to the deleterious effects of aging.

Materials and methods

Animals

In order to optimize sampling from our animal colony for the assessment of vascular density with aging, we used young adult (3–5.5 months old, mean = 3.5, male: n = 20, female: n = 5) and aged (16.5–22 months old, mean = 19.3, male: n = 40) mice. Since we had very few aged female mice in our colony, we could not make meaningful sex-based comparisons in our study. The mice were derived from three different strains: (a) C57BL/6J (young adult: n = 36, aged: n = 9), (b) *Tek*-GFP (young adult: n = 4, aged: n = 4) (The Jackson Laboratory, 003658), and (c) *Tek*-CreER^{T2} X *Kdr*$^{+/fl}$ (aged: n = 12) [*Tek*-CreER^{T2} line[25] (EMMA 00715) bred with *Kdr*$^{fl/fl}$ line[26]] strains. Statistical comparisons revealed no difference in capillary density between aged C57BL/6J mice and *Tek*-CreER^{T2} X *Kdr*$^{+/fl}$ mice (Unpaired with Welch's correction for unequal variances $t_{(9.781)}$=0.8246, p = 0.4293), therefore data from these two strains were pooled. The *Tek*-GFP aged animals were strain-matched with an equal number of young and aged *Tek*-GFP mice. Since an age-by-strain two-way ANOVA revealed no significant age–strain interaction (two-way ANOVA interaction $F_{(1,65)}$=0.1673, p = 0.6838), *Tek*-GFP mice were also pooled with the rest of the mice in both young and aged groups. All mice were housed under a 12-hour light/dark cycle with *ad libitum* access to water and standard laboratory diet. All experiments were conducted according to the guidelines set by the Canadian Council of Animal Care and approved by the University of Victoria Animal Care Committee (protocol 2016-016). Reporting of this work complies with ARRIVE guidelines.

Tissue preparation, imaging and vessel analysis

For vessel density quantification, lysine fixable FITC dextran (100 µL; 2% w/v in 0.9% saline; ThermoFisher, molecular weight 40 kDa, D1845) was intravenously injected and left to circulate for 8 min prior to decapitation. The brain was extracted, bisected along the midline and fixed in 4% paraformaldehyde (PFA) in 0.1 M phosphate buffered saline (PBS) overnight at 4°C before being transferred to 0.1 M PBS. Brains were sectioned in the coronal plane at 50 µm thick using a Leica vibratome (T1000). Every sixth section was mounted on a gelatin-coated slide, and coverslipped with Fluoromount G (ThermoFisher, 00-4958-02). FITC-labeled vessels in the brain were imaged using a 488 nm laser on an Olympus confocal microscope with a 10× objective (NA 0.40). Since aging brains can exhibit autofluorescence in extra-vascular spaces which needs to be accounted for, we excited samples with a 561 nm laser and collected light using a Texas Red emitter filter (575–675 nm). Confocal image stacks were collected in 4 µm z-steps at a pixel resolution of 1.242 µm/pixel. Two to three image stacks for each of the 15 brain regions sampled were captured

in each animal within the colored boundaries outlined in Supplementary Figure 1. Care was taken to ensure sampling at rostral-caudal levels was comparable between groups.

Images were analyzed using a custom-built macro for FIJI-ImageJ (version 1.52e). First, the macro worked by creating a maximal intensity image projection of eight images from each stack in both green (FITC-vessel signal) and red channels (autofluorescent background signal). Autofluorescent signal was corrected for by subtracting images in the red channel from the green channel (Figure 1(a)). In order to optimize the automated detection of vessel segments in the image, we used a WEKA Trainable Segmentation machine learning plugin from ImageJ and trained our macro using 20 separate images with user defined vessel segments.[27] Once the WEKA Trainable Segmentation plugin successfully differentiated fluorescent signal in vessels from background (see yellow and pink outline in Figure 1(a)), images were segmented and then skeletonized. In order to correct for small gaps in connected capillaries (caused by dips in fluorescent plasma signal within the vessel), capillary end segments were connected if they were within 12 μm of each other and within a linear slope of 60° on either side of the fitted straight-line segment. A slope of 60° was determined empirically as it did not result in false positive connections given that connected capillaries do not often change direction by >60 degrees in a 12 μm segment of vessel. Dependent variables that were measured included total vascular length, mean vessel diameter (total area of dye/vascular length), and mean tortuosity (arc-chord ratio for all segments). Since signal segmentation tends to overestimate vessel area which was used to generate width measurements, we needed to calculate a transforming factor. This was done by measuring the full width at half maximum (FWHM) diameter of randomly selected vessels (9–11 vessels in five animals) in both the raw maximum projection and the segmented image. Segmented image-derived diameters were calibrated by dividing by the transforming factor of 2.056 (i.e. the average ratio between diameters in each image). To validate our automated analysis, estimates of vessel density and tortuosity generated from our custom macro were compared to ground truth, user defined estimates generated by an independent and blinded observer. User-measured vessel length was plotted against macro-generated length and linear regression was performed (Figure 1(b)). The equation of the regression line was used to transform the vascular length measurements generated by the macro (Figure 1(b) and (c)). Similarly, tortuosity (measured as Arc-chord ratio, Figure 1(d)) from user-drawn images was plotted against macro-generated tortuosity (Figure 1(e) and (f)). To ensure that changes in tortuosity could not arise from changes in diameter, the difference between the hand-drawn and macro-generated tortuosity was plotted against the mean capillary diameter in each image and regression was performed (Figure 1(g)).

Some confocal image stacks could not be properly analyzed by our automated program due to uneven signal across the specimen (e.g. caused by poor sectioning). Therefore, out of 3022 image stacks collected, 39 were identified as an outlier (1.29% of total) by the Repeated Grubbs Test and excluded from the analysis.

Analysis of specific brain regions was restricted based on a user-defined region of interest (ROI) that excluded vessels >20 μm diameter. We should note that larger vessels (8–20 μm diameter) were included in the analysis; however, a random sample of images showed that vessels >8 μm diameter accounted for approximately just $4 \pm 1.5\%$ (mean±SD) of the total vascular length ($n = 5$). Given this information, age-related changes in vascular structure are overwhelmingly represented (~96%) by changes at the capillary level.

Pockets of vessel sparse sub-regions were quantified using a custom-built macro for FIJI that subdivided image skeletons into 211×211 μm squares (44,550 μm^2) and reported local vascular density (m/mm^3). The fraction of subsections with less than 50% of the mean vascular density for that specific brain region (for young adult mice) were reported.

Capillary obstruction model and microsphere density analysis

To assess region specific differences in susceptibility to capillary obstructions, we used male young adult C57BL/6J mice (3–4 months old, mean = 3.4, 30 min: $n = 16$, 3 day: $n = 15$). Mice were briefly (<15 min) anesthetized with 1.5% isoflurane gas mixed in medical grade air with body temperature maintained at 37°C. As previously described,[24] we intravenously injected 100 μL of 4 μm diameter fluorescent microspheres (2% solids; Life Technologies FluoSpheres sulfate) to induce capillary obstructions. Red or green fluorescent microspheres (ThermoFisher catalog# F8858 and F8859) were injected 3 days or 30 min, respectively prior to euthanasia to estimate transient and long-lived capillary obstructions. Mice recovered under a heat lamp immediately after injection before being returned to their home cage. Mice were killed from an overdose of sodium pentobarbital, the brain was immediately extracted, then bisected and each hemisphere immersed in 4% PFA overnight before being transferred to 0.1 M PBS. We sectioned brains on a Leica vibratome (T1000) to make 100 or 50 μm-thick coronal sections. Every third section was mounted onto a gelatin-coated slide, and cover-slipped with

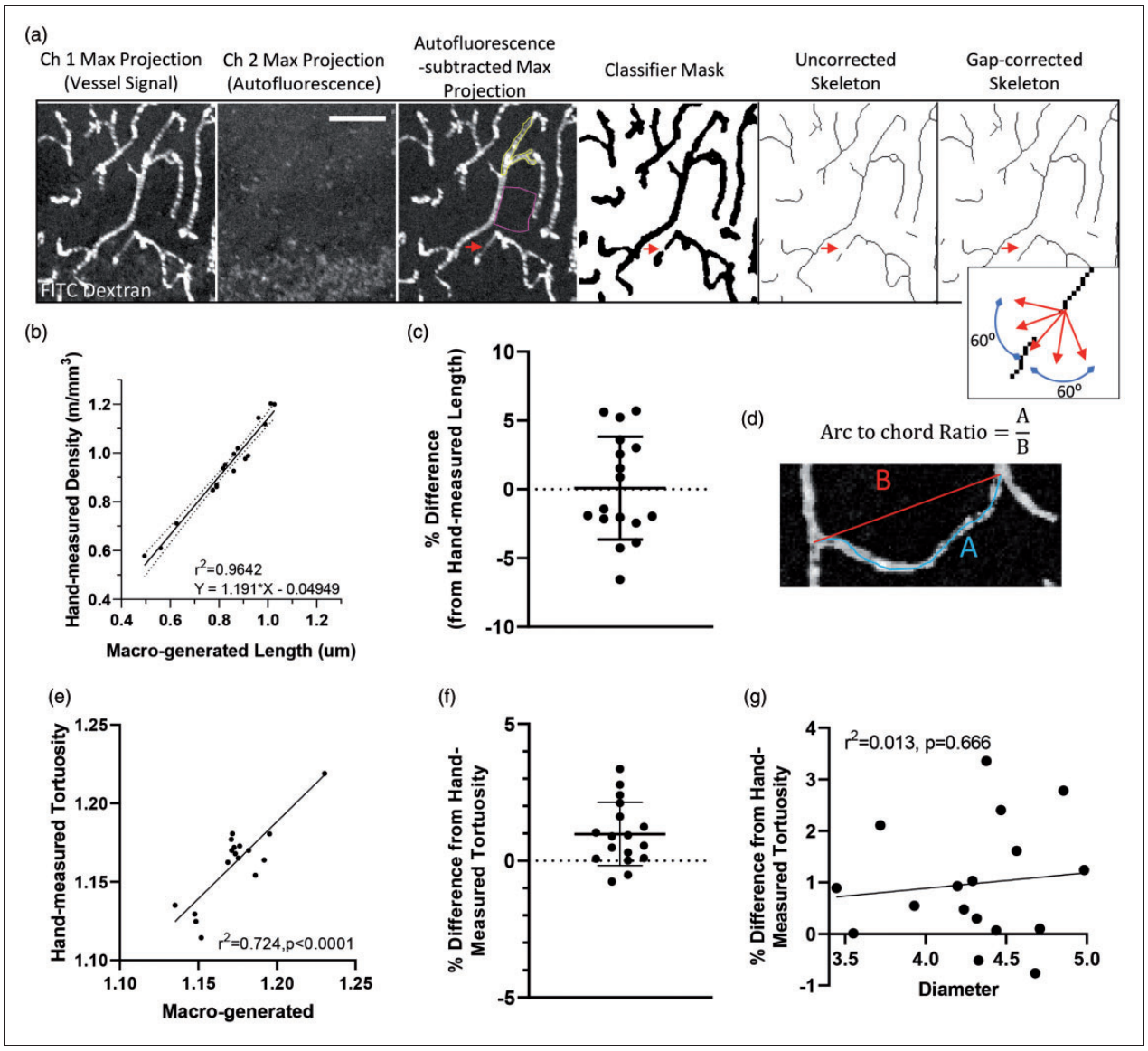

Figure 1. Validation of automated approach for analyzing vessels. (a) Confocal image stacks from channel 1 (FITC-labeled vessels) and 2 (tissue autofluorescence) were first maximally projected with autofluorescent signal subtracted from the original image. Using a supervised learning plugin to segment fluorescent signal from background (signal outlines in yellow with background in pink), the image was skeletonized. Gaps in vessel signal (red arrows) were corrected if capillary segments were within 12 μm of each other and within a linear slope of 60° on either side of the fitted straight line segment (see inset). Scale bar = 50 μm. (b) Vessel lengths for each image were estimated from the automated macro and then plotted relative to lengths generated from a blind observer. Note the extremely tight relationship (r^2=0.964) between automated and observer defined estimates. (c) Difference in lengths estimated by the two approaches after translation of macro-generated values (mean ± S.D.). (d) Image illustrating arc-chord ratio, a measurement of tortuosity. (e) Tortuosity measurements for each image (n = 17) were estimated from the automated macro and then plotted relative to those generated from a blind observer. (f) Difference in tortuosity estimated by the two approaches (mean ± S.D.). (g) Regression analysis of mean vessel diameter generated for the 17 images plotted against the difference in tortuosity generated by the two approaches. This analysis shows that vessel diameter does not influence the macro-generated estimate of tortuosity.

Fluoromount G. Ultra-bright fluorescent microspheres were imaged on an upright wide-field Olympus BX51 microscope with a 2× Olympus Plan objective (NA = 0.05, 228 pixels/mm) using GFP and Cy3 excitation/emission filter sets on an Olympus DP73 digital CCD camera using CellSens software. Images were taken from every third section from approximately +2.7 mm to −3.5 mm from bregma.[28] Using a custom-built macro for FIJI, ROIs were manually drawn on each image over every present brain region, as shown in Supplementary Figure 1 and guided by the Franklin and Paxinos Mouse Brain Atlas.[28]

Microspheres were automatically counted in each ROI using a threshold of 2/3 maximum pixel intensity. The density of obstructions within each brain region was expressed as # obstructions per meter length of capillary.

To test the hypothesis that regional microvascular obstruction rates would correlate with the magnitude of region-specific vessel loss with aging, a linear regression was calculated, plotting mean vascular length loss against microsphere density. Density values for each region were normalized within each animal and expressed as % difference relative to the mean microsphere density across all brain regions. The obstruction clearance rate was based on the difference between 30 min and 3-day obstruction densities in each region.

Cortical and callosal thickness analysis

Cortical thickness was measured in FIJI by drawing straight lines perpendicular from the cortical surface to the white matter in six places: retrosplenial, visual, peri-rhinal, insular, motor and forelimb somatosensory cortex. The thickness of corpus callosum was measured by plotting straight dorsal-ventral (y-axis) lines for each pixel in the x-axis (white matter runs parallel to x-axis). Every third section within a region was sampled to estimate thickness.

Code accessibility

Custom FIJI macros can be freely accessed on GitHub at https://github.com/bschager/Microvessel-Density-Analysis.[29] Image classifier files are available from the authors on demand.

Statistics

All statistical analyses were performed using GraphPad Prism 8 using an alpha value of 0.05. A multivariate mixed analysis was used where appropriate. Two-way mixed ANOVA was used when there were no missing values, while a mixed model was fitted to the data (using Restricted Maximum Likelihood) when there were missing values in the dataset. Where the assumption of sphericity was not met, the Geisser-Greenhouse correction was used. Post-hoc comparisons were performed using Sidak's multiple comparisons test for multi-variate mixed-model analyses and paired t-tests for univariate mixed-model analyses. Repeated measures ANOVA was used to test for region-related differences in microsphere clearance rates. Data are presented as mean $\pm$ 95% confidence interval (CI), unless otherwise stated. Supplementary Table 1 provides detailed results of the post-hoc tests comparing young adult and aged animals.

Outliers were detected using Grubbs test, with an alpha value of 0.05. For example, 4/1298, 2/431, and 2/848 data points were identified as outliers for vessel density, cortical thickness, and tortuosity, respectively. When analyzing the relationship between vessel loss and obstruction rate, retrosplenial cortex was identified as an outlier at both 30 min and 3-day time points and excluded from the linear regression analysis.

Results

Vessel loss with aging occurs in a region-specific manner

In order to determine the magnitude of vessel loss with aging and whether certain brain regions were more vulnerable than others, we intravenously injected young adult and aged mice ($n = 40$ and 25, respectively) with fixation-compatible FITC dextran and then generated over 3000 confocal image stacks of fluorescently labeled blood vessels in 15 different brain regions (Figure 2). To analyze this large data set, we generated an automated macro for estimating vessel length that very closely matched estimates produced by a blinded observer (Figure 1(b) and (c), $r^2=0.964$; mean difference of $0.08 \pm 3.74\%$).

A mixed model two-way ANOVA revealed a significant main effect of age ($F_{(1,63)}= 27.08$, $p < 0.0001$), brain region ($F_{(14,821)}= 664.8$, $p < 0.0001$), and a significant age by region interaction ($F_{(14,821)}= 3.870$, $p < 0.0001$). As shown in Figure 3(a) and (b) and Supplementary Table 1, vessel loss (displayed as m/mm^3 and % vessel loss) with aging was not uniform across brain regions. Post-hoc analysis revealed significant loss of vessel length in 7 out of the 15 regions sampled. The area with the greatest magnitude of vessel loss was the corpus callosum, exhibiting a $\sim$26% reduction in vascular density with age (Figure 3(a) and (b)). In the cortex, the motor, peri-rhinal/ecto-rhinal, forelimb somatosensory and retrosplenial areas exhibited significant loss of vessel length (mean= 10.29%), while frontal cortex trended towards loss ($t_{(54.82)}= 2.907$, $p = 0.0759$). By contrast, the insular ($t_{(53.40)}= 1.470$, $p = 0.9087$) and visual cortex ($t_{(56.55)}= 1.001$, $p = 0.9970$) did not show any loss (Figure 3(a) and (b)). Subcortically, significant loss of vessel length was also observed in the hippocampus and hypothalamus (Figure 3(a) and (b); mean= 10.47%) with a trend in the striatum ($t_{(55.56)}= 3.002$, $p = 0.0582$) and substantia nigra ($t_{(56.27)}= 2.880$, $p = 0.0810$). However, there were no changes in thalamus ($t_{(58.22)}= 2.342$, $p = 0.2904$) or lateral amygdala ($t_{(41.76)}= 0.201$, $p > 0.9999$).

Given our broad sampling of brain regions, we next attempted to determine if there were supra-regional

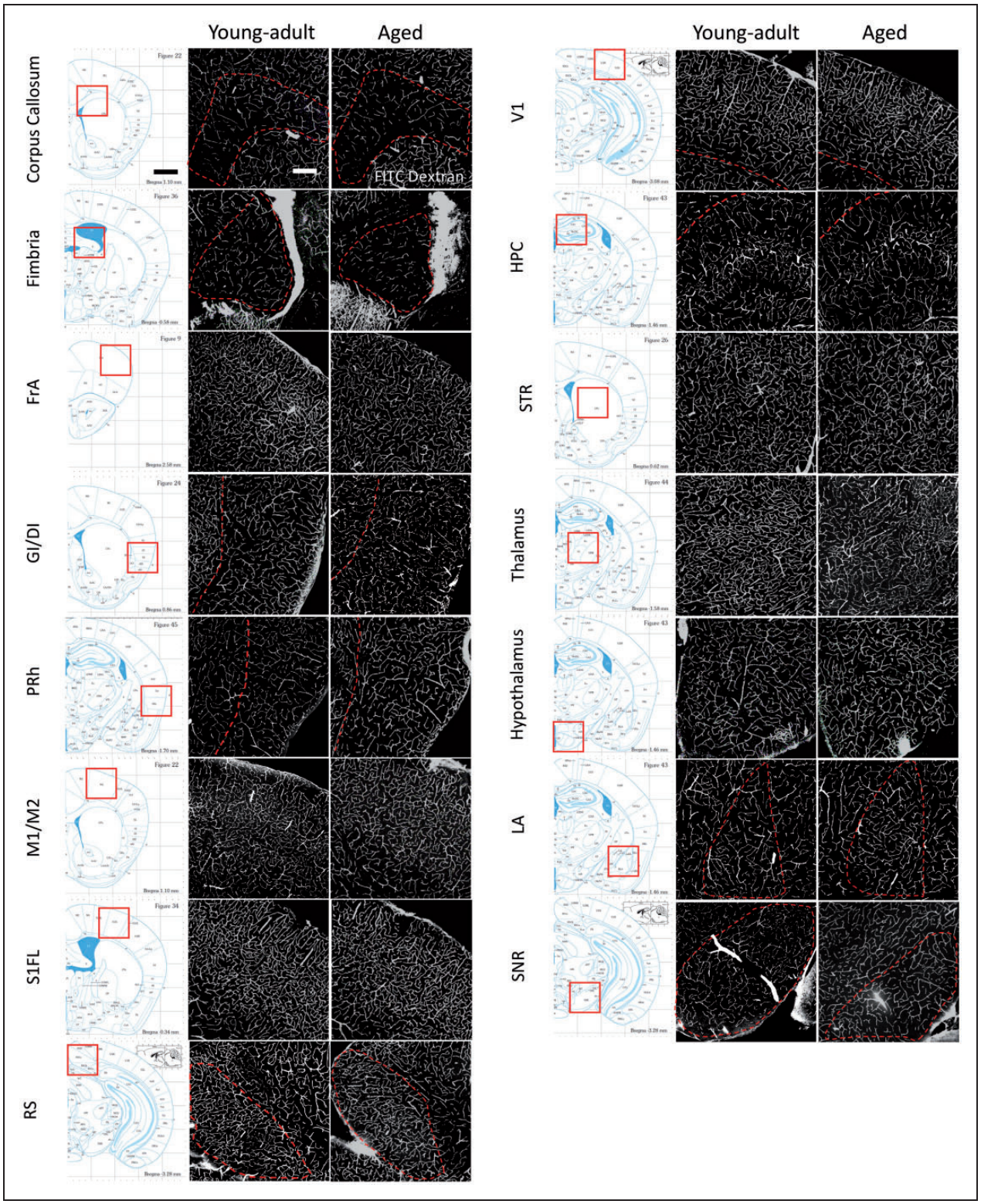

Figure 2. Representative images of the vasculature across different brain regions in young adult and aged mice. The location of each brain region analyzed is illustrated by the stereotaxic atlas image shown in the left pane. On the right are confocal image projections showing FITC-labeled vessels in young adult (3–5.5 months old) and aged mice (16.5–22 months old). Image contrast was adjusted for the sake of clarity. Scale bar = 200 μm. FrA: frontal association cortex; GI/DI: granular/dysgranular insular cortex; PRh/Ect: peri-rhinal cortex/Ecto-rhinal; M1/M2: primary/secondary motor cortex; S1FL: primary forelimb somatosensory cortex; RS: retrosplenial cortex; V1: primary visual cortex; HPC: hippocampus; STR: striatum; LA: lateral amygdaloid nucleus; SNR: substantia nigra reticulate.

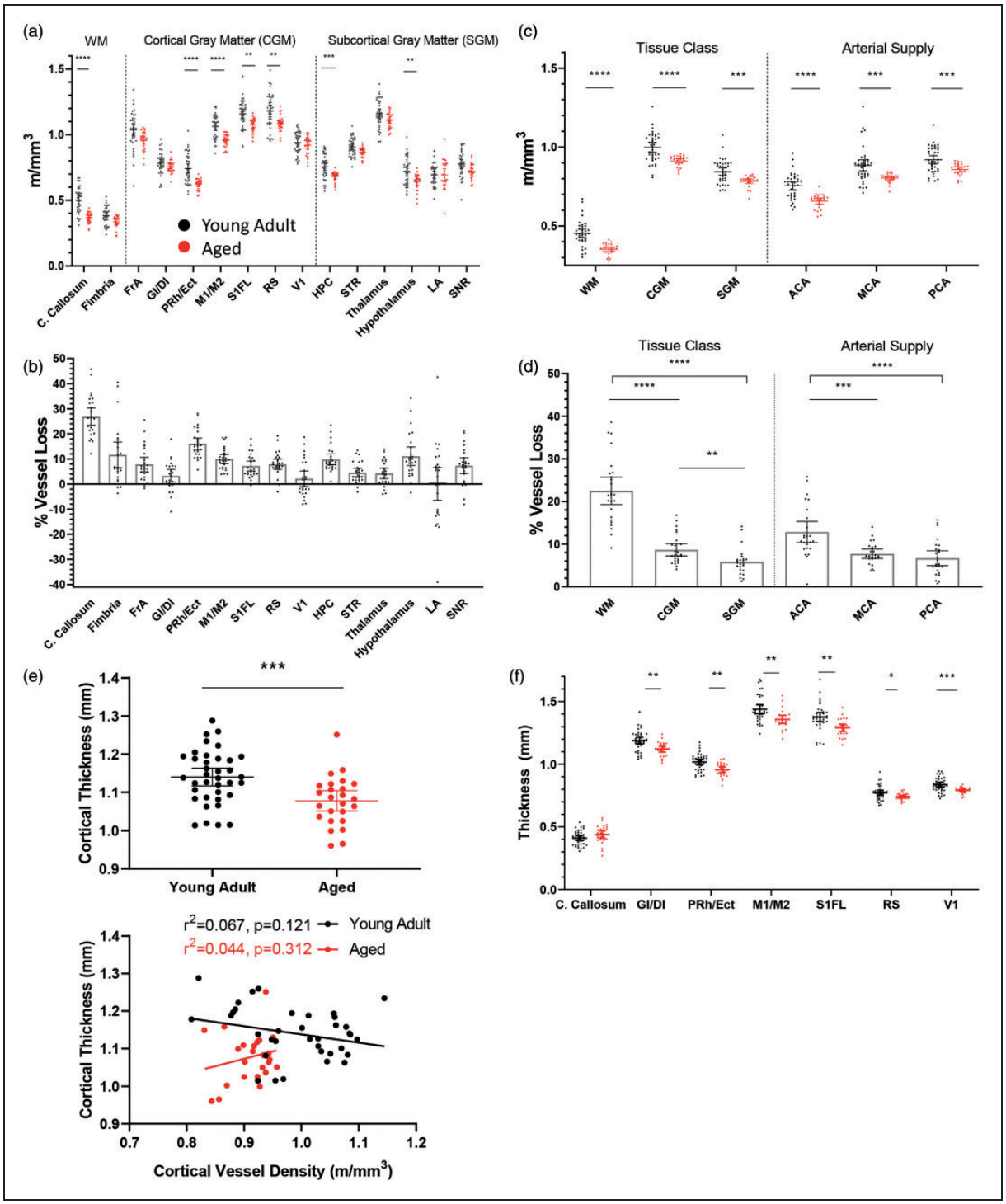

Figure 3. Loss of vessel length with aging is brain region specific. (a) Quantification of vessel length per cubic volume of tissue in each region in young adult (black dots; n = 40 mice) and aged mice (red dots; n = 25 mice). (b) Relative magnitude of age-related vessel loss in each brain region. (c) Graphs show vessel length changes in young adult and aged mice as a function of tissue class or arterial supply. (d) Age-related vessel loss binned according to tissue class or arterial supply. (e) Graph showing differences in average cortical thickness with aging (top panel) and linear regression analysis (bottom panel). Note no systematic relationship between cortical thickness and vessel length density measurements in young adult or aged mice. (f) Graph showing age related changes in cortical, but not callosal thickness. Data in (a), (c) and (f) were analyzed by fitting a mixed model to approximate two-way mixed ANOVA followed by Sidak's multiple comparisons test. Data in (d) were analyzed by fitting a mixed model to approximate repeated measures ANOVA followed by post-hoc paired t-tests. Data in (e) were analyzed with an unpaired t-test. Error bars: mean ± 95% CI. ****$p < 0.0001$, ***$p < 0.001$, **$p < 0.01$, *$p < 0.05$. WM: white matter; CGM: cortical grey matter; SGM: subcortical grey matter.

patterns of age-related vessel loss. For example, white matter is known to be susceptible to degeneration with aging and is thought to be an important factor in cognitive decline.[30–33] Additionally, it is conceivable that vessel loss may vary as a function of vascular perfusion territory given inherent territorial differences in the incidence of stroke or collateral circulation.[34,35] Therefore, we assigned each brain region area a classification based on tissue type (white matter vs. cortical grey vs. subcortical grey matter) or major supplying cerebral artery and assessed vascular loss. Classifications and references for assigning brain regions to a specific perfusion territory are detailed in Supplementary Table 1. As shown in Figure 3(c), vessel length was significantly lower in aged mice in all tissue classes (Main effect of Age for Tissue Class: $F_{(1,63)}= 30.63$, $p < 0.0001$) and arterial supply zones ($F_{(1,63)}= 24.63$, $p < 0.0001$), reflective of the general trend for vessel density to decrease with age. However, comparing the percent vessel loss within these categories revealed differences. For tissue class (Figure 3(d)), paired t-test revealed that vessel loss was significantly greater in white matter (WM) compared to cortical gray matter (CGM) ($t_{(24)}= 11.64$, $p < 0.0001$) and subcortical gray matter (SGM) ($t_{(23)}= 12.65$, $p < 0.0001$), while cortical gray matter vessel loss was greater than subcortical gray matter ($t_{(23)}= 3.738$, $p = 0.0011$). For arterial supply (Figure 3(d)), loss of vessel length was significantly greater for anterior cerebral artery (ACA) fed territories than for middle (MCA; $t_{(23)}= 4.324$, $p = 0.0003$) or posterior-fed cerebral arteries (PCA; $t_{(24)}= 6.744$, $p < 0.0001$). Lastly, we assessed cortical thickness in select regions ($n = 6$ regions) and found that cortical thickness was significantly reduced in aged mice (Figure 3(e), top panel; $t_{(60)}= 3.562$, $p = 0.0007$). However, cortical thickness had no relationship with vessel length measurements (Figure 3(e), bottom panel), implying that slight shrinkage of the brain with age did not systematically influence our length measurements. Breaking thickness measurements down by region revealed a uniform reduction across cortical areas, but not in the corpus callosum (Figure 3(f)). Linear regression did not reveal any relationship between vessel loss and changes in thickness ($r^2=0.08797$), further showing that possible volume reductions did not systematically influence length measurements. Collectively these results show that the loss of vessel length with aging is a heterogeneous phenomenon with certain brain regions showing greater vulnerability than others.

Age-related changes in vessel tortuosity and diameter

Next, we wanted to determine if the loss of vessel length with aging could be explained or compensated for by changes in vessel structure such as tortuosity or width. We estimated mean vessel tortuosity, measured as the arc-chord ratio (Figure 1(d), increasing values indicate greater tortuosity) from two to three images in each region per animal. Tortuosity measurements generated from our custom macro were cross-referenced and validated using measurements generated by a blinded observer (Figure 1(e) and (f)). Further, to ensure that our tortuosity measurements were not artificially influenced by vessel diameter, we performed a linear regression analysis and found no relationship between these variables (Figure 1(g)). Our analysis of tortuosity revealed a significant main effect of age ($F_{(1,59)}= 15.19$, $p = 0.0003$), brain region ($F_{(6.542,353.7)}= 16.87$, $p < 0.0001$), and age by region interaction ($F_{(14,757)}= 4.383$, $p < 0.0001$). Specifically, tortuosity increased with age in frontal cortex, visual cortex, hippocampus, and amygdala (Figure 4(a)). Next, we used a linear regression analysis to determine whether vessels in brain regions that were more prone to loss with aging were: (a) more tortuous in young adult mice or (b) more likely to show a change in tortuosity with age. Our analysis revealed no significant systematic relationship between vessel loss and young adult tortuosity (Figure 4(b)). However, we found a moderate relationship between vessel loss and areas that show a change in tortuosity with age (Figure 4(c)), though this relationship was skewed by the corpus callosum (relationship with callosum: $r^2=0.4659$, without callosum: $r^2=0.1195$). Vessel diameter also showed age and region specific changes (main effect of age: $F_{(1,59)}= 28.72$, $p < 0.0001$; brain region: $F_{(3.053,165.5)}= 22.97$, $p < 0.0001$; age by region interaction: $F_{(14,759)}= 6.133$, $p < 0.0001$), with the general trend for vessel diameter to increase with age (Figure 4(d)). We found a very weak relationship between vessel loss and vessel diameter in young animals (Figure 4(e)), and no systematic relationship between regional vessel loss and changes in vessel diameter with aging (Figure 4(f)). These findings reveal that vessel tortuosity and width change in a region-specific manner with aging, but possess little predictive value for the magnitude of vessel loss.

Zones of vessel sparse regions increase with age

A recent oxygen imaging study found micro-pockets of hypoxic brain tissue (up to 200 μm in size) in ~24 month-old mice.[36] One possible explanation for this local hypoxia is that aging may increase the likelihood of vessel sparse micro-zones, especially if vessel loss exhibits some degree of clustering. To test this, we subdivided vascular skeletons into 211×211 μm grids and quantified the number of pockets that had less than 50% of the mean vascular density for the brain region examined (Figure 5(a)). Our analysis revealed a

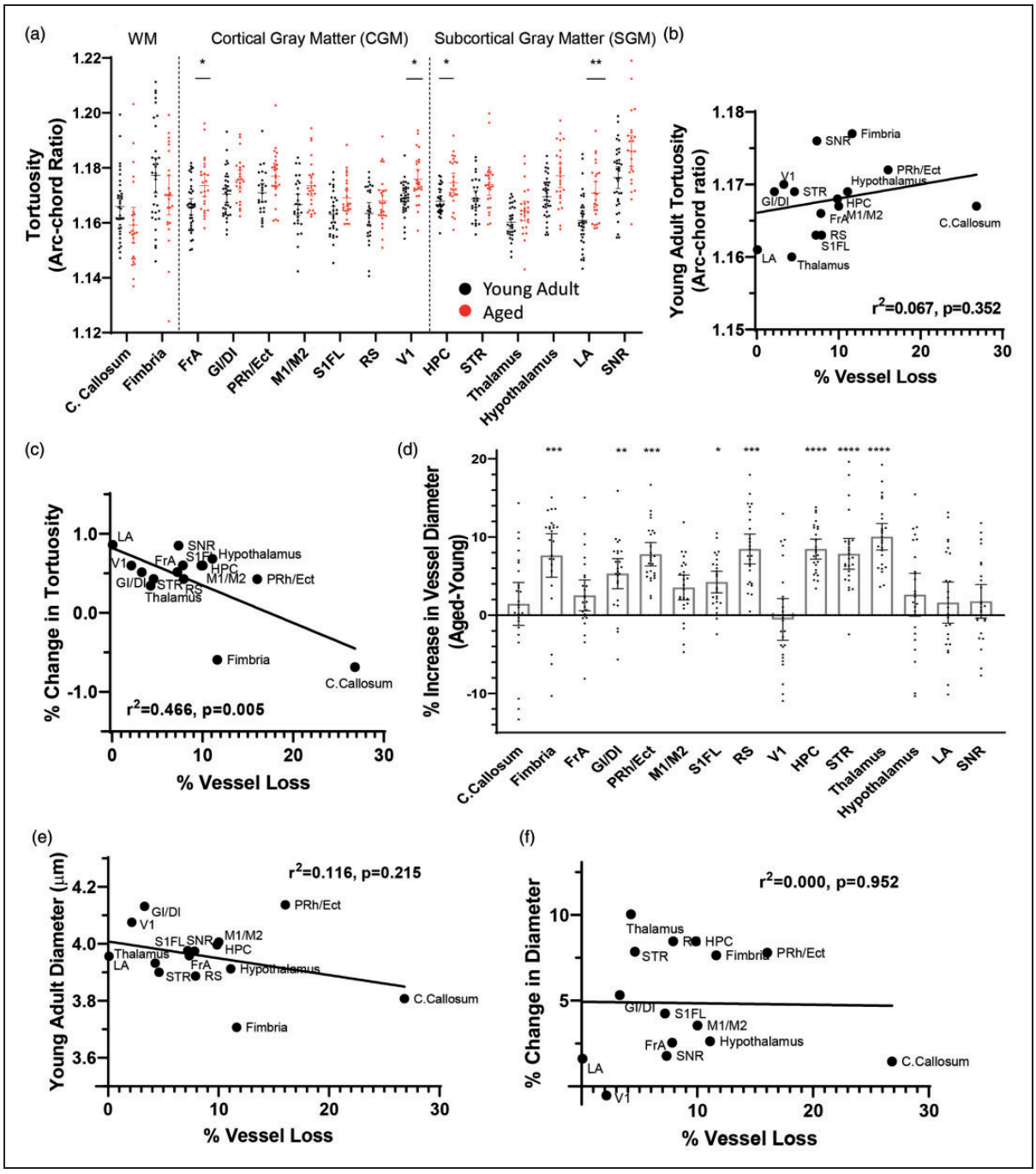

Figure 4. Age-related changes in vessel tortuosity and diameter. (a) Quantitative differences in tortuosity across different brain regions in young adult and aged mice. Regression analysis did not reveal any relationship between age-related vessel loss and the extent of tortuosity in specific brain regions of young adult mice, (b) but a moderate relationship was found in the % change with aging (c). (d) Graphs show age-related changes in vessel width in each brain region. There was a very weak relationship between regional vessel loss and diameter in young mice (e), and no relationship between regional vessel loss and changes in vessel width with aging (f). Data in (a) and (d) were analyzed by fitting a mixed model to approximate two-way mixed ANOVA followed by Sidak's multiple comparisons test. Error bars: mean ± 95% CI. ****$p < 0.0001$, ***$p < 0.001$, **$p < 0.01$, *$p < 0.05$.

significant main effect of age ($F_{(1,59)}$= 11.58, $p = 0.0012$), brain region ($F_{(4.003,217.0)}$= 59.69, $p < 0.0001$) and age by region interaction ($F_{(14,759)}$= 8.508, $p < 0.0001$). As shown in Figure 5(b), two areas in particular exhibited a significant increase in the frequency of vessel sparse zones: the corpus callosum ($t_{(55.44)}$= 4.844, $p = 0.0002$) and the substantia nigra ($t_{(34.42)}$= 4.535, $p = 0.0010$). When grouped by

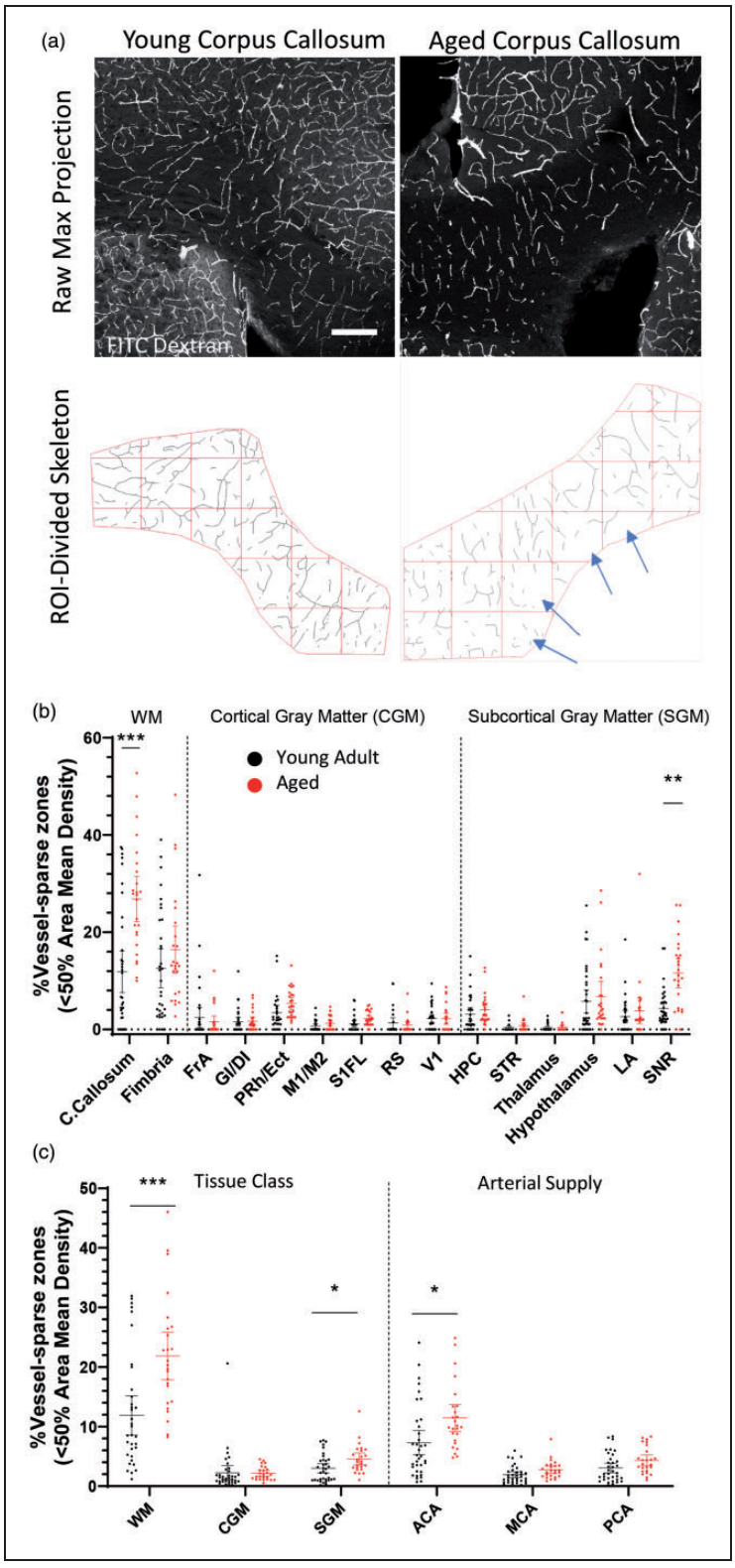

Figure 5. Pockets of vessel sparse zones in the aged brain. (a) Confocal image projections showing FITC-labeled vasculature in the corpus callosum in young adult and aged mice (top row), and corresponding skeletonized images illustrating how vessel sparse microzones were analyzed (bottom panel). Scale bar = 200 μm. Graphs show the % of vessel sparse zones in young adult and aged mice in each brain region (b) or according to tissue class or arterial supply (c). Data in (b) and (c) were analyzed by fitting a mixed model to approximate two-way mixed ANOVA followed by Sidak's multiple comparisons test. Error bars: mean ± 95% CI. ****$p < 0.0001$, ***$p < 0.001$, **$p < 0.01$, *$p < 0.05$.

tissue class or arterial territory (Figure 5(c)), white matter, subcortical gray matter, and ACA-supplied tissues showed a statistically significant age-related increase in the prevalence of vessel sparse pockets (WM: $t_{(51.86)}= 3.962$, $p = 0.0007$; SGM: $t_{(50.02)}= 2.560$, $p = 0.0401$; ACA: $t_{(54.90)}= 2.769$, $p = 0.0228$).

Vulnerability to long lasting capillary obstructions is predictive of vessel loss with aging

Previous work from our lab has shown that long-lasting naturally occurring or microsphere-induced capillary obstructions result in vessel pruning in ~30% of cases.[24] To help explain why some brain regions might show greater vessel loss with aging than others, we hypothesized that these vulnerable regions would be more susceptible to capillary obstructions. Therefore, we intravenously injected 4 μm diameter red or green microspheres into young adult mice 30 min and 3 days before extracting the brain (Figure 6(a)). We reasoned that the 30 min time point would provide an estimate of short-lived (likely transient) obstructions whereas the 3-day time point would reflect persistent, long lasting obstructions. Figure 6(b) demonstrates the presence of microspheres within cerebral vessels, obstructing the lumen of capillaries. We should note that microspheres did not lead to ruptured vessels as they were not found in extravascular spaces (Figure 6(b)), nor were microglia aggregated around them (Figure 6(c)).[24] Quantification of microsphere density in different brain regions from 30 min and 3-day time points revealed a heterogenous distribution (Figure 6(d); Repeated measures ANOVA of brain region at 30 min with RS: $F_{(4.035,60.52)}= 19.54$, $p < 0.0001$ and 3 days: $F_{(4.235,59.29)}= 7.890$, $p < 0.0001$). This distribution remained regionally heterogeneous even after excluding retrosplenial cortex from the analysis (Repeated measures ANOVA of brain region at 30 min without RS: $F_{(3.532,52.97)}= 10.43$, $p < 0.0001$ and 3 days: $F_{(3.826,53.56)}= 3.239$, $p = 0.0202$). As indicated in Figure 6(e), the overwhelming majority of microspheres were cleared from the brain at both 30 min and 3-day time points (~95% on average across all regions). By calculating the % clearance rate (1–3 day density/30 min density), one can note significant region-specific variability in clearance rates (Figure 6(e); Repeated measures ANOVA $F_{(4.265,59.71)}= 3.840$, $p = 0.0066$). To determine whether obstruction density at 30 min or 3 days was predictive of region-specific vessel loss with aging, we performed linear regression analyses between the mean magnitude of vessel loss for each area and normalized obstruction rates in young adult animals (Figure 6(f)). In addition, we performed a regression analysis for vessel loss and each region's clearance rate (Figure 6(g)). Our analysis revealed a significant positive relationship between long lasting obstructions found in each region at 3 days (but not 30 min) and the degree of microvascular loss with aging (Figure 6(f), left panel). Similarly, brain regions that were better at clearing obstructions (indicated by higher clearance rate in Figure 6(g), left panel) were less susceptible to age-related vessel loss. Parsing out these relationships according to tissue class, we found stronger correlations for vessel loss in cortical gray and white matter regions (Figure 6(f) and (g), middle panel), than subcortical gray matter (Figure 6(f) and (g), right panel). These results indicate that brain regions with an increased susceptibility to long-lasting capillary obstructions (and those less able to clear them) are more likely to experience greater vessel loss with aging.

Discussion

The loss of brain microvessels with aging has been reported in several species including humans (see Supplementary Table 2). However to our knowledge, no previous study had examined this phenomenon in more than a couple brain regions (see Supplementary Table 2),[37–39] therefore a systematic assessment of brain region-specific vulnerability to vessel loss with aging was lacking. We believe this was an important question to address because if there are strong brain region specific patterns in vessel loss, it may help explain why certain cognitive and sensory-motor functions are more susceptible to aging than others. Here we assessed 15 different regions in the mouse brain and show that age-related microvascular loss occurs in a heterogeneous manner. Our data show that motor and somatosensory cortex, but not visual cortex, undergo significant vessel loss with aging, which agrees with previous studies in both mouse[24] and rat.[37,38] In accordance with previous reports,[37–39] the hippocampus and white matter tracts of the corpus callosum show pronounced age-related vessel loss. By including largely unexplored limbic cortical or sub-cortical regions in our study like the retrosplenial, insular, peri-rhinal cortex, amygdala, thalamus and substantia nigra, our data reveal that limbic cortical areas (retrosplenial and peri-rhinal cortex) exhibit significant vessel loss, whereas subcortical regions such the thalamus, striatum and amygdala were more resilient. Despite the scant literature in sub-telencephalic regions, a post-mortem study examining the lateral geniculate nucleus of the thalamus also found very little change in vessel length or number with aging.[40] Collectively, these findings strongly support the idea that rarefaction of microvascular networks are differentially affected by aging.

Our findings also suggest regional differences in vascular loss based on tissue class and perfusion supply.

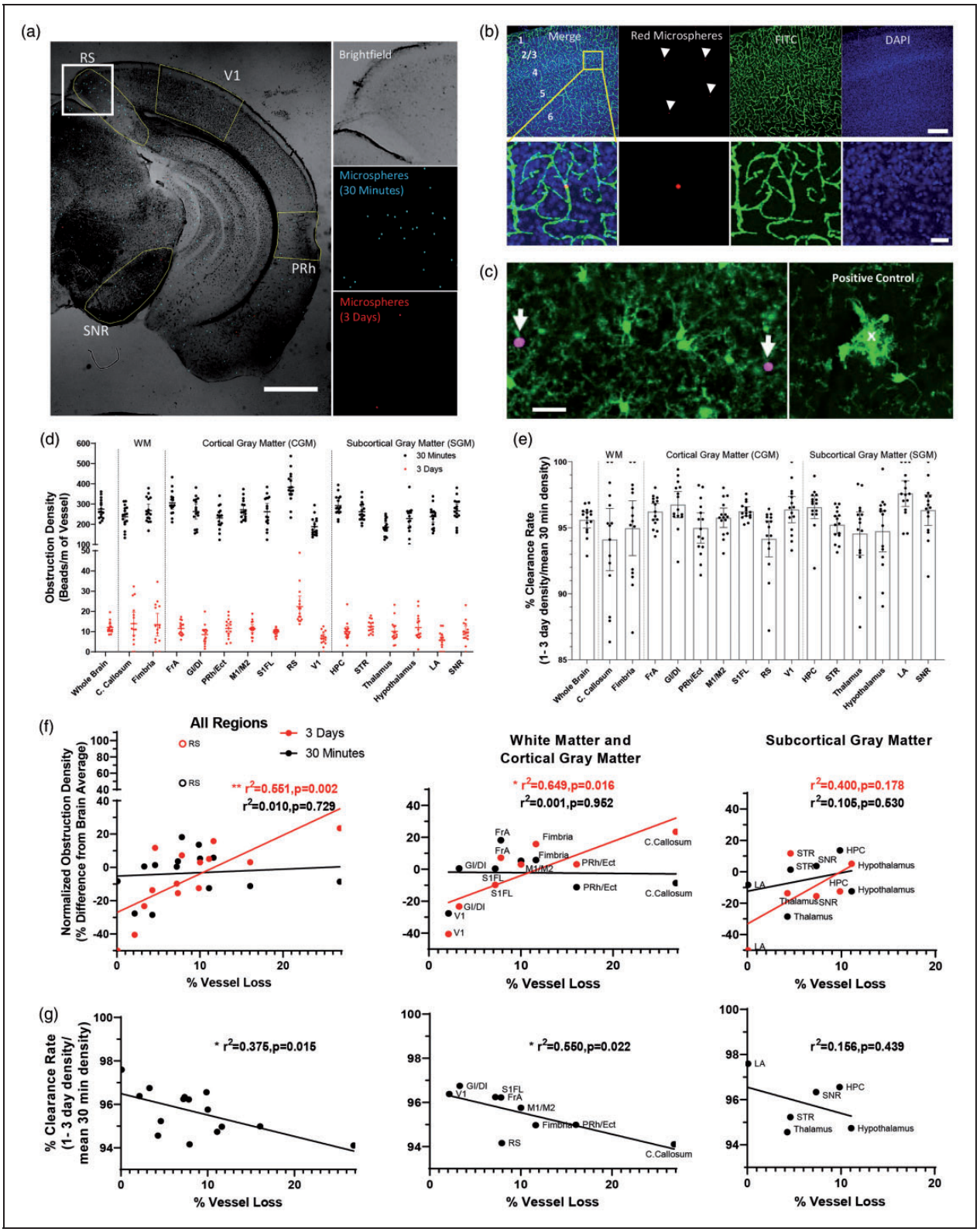

Figure 6. Regional vulnerability to capillary obstructions is predictive of vessel loss with aging. (a) Widefield images of coronal brain sections showing transient (blue colored microspheres) and long-lasting capillary obstructions (red colored microspheres) injected 30 min or 3 days, respectively, prior to brain extraction. Scale bar = 1 mm. (b) Images show red microspheres reside within FITC-labeled capillaries in the forelimb somatosensory cortex. Scale bar = 200 μm (top row), 20 μm (bottom row). (c) Confocal images show no preferential aggregation of GFP-labeled microglia around microspheres, suggesting that microspheres do not cause

(continued)

Indeed, when vessel loss was grouped according to tissue class (white matter vs. cortical vs. subcortical grey matter), white matter was most vulnerable while subcortical grey matter was the least affected. Furthermore, white matter was one of the only regions studied to show pockets of vessel sparse zones. The finding that white matter is susceptible to vessel loss is perhaps not surprising since white matter atrophy is associated with aging, especially when compounded with dementia or vascular risk factors such as diabetes, hypertension and hypercholesterolemia.[8,31,41] The directionality of this relationship is not fully understood as white matter degeneration could lead to capillary rarefaction or the loss of capillaries could exacerbate white matter degeneration by reducing perfusion and increasing the risk of infarction, as capillary dysfunction is known to do.[9] As noted by Brown and Thore,[15] the blood supply for anterior white matter tracts (similar to the location of corpus callosum analyzed in the present study) is perilous as it arises from the distal ends of the anterior cerebral artery. A possible consequence is that capillary blood flow would be more susceptible to global perfusion changes[42] that could increase the risk of capillary stalls/obstructions (caused by blood cells, fibrin, cholesterol). In fact, the relative distance of each brain region to the proximal branches of a cerebral artery may partially explain why more distal perfusion regions like the somatosensory, motor and retrosplenial cortices exhibited vessel loss with aging whereas more proximal subcortical regions such as the striatum and thalamus, did not.

Another related factor influencing vessel loss appears to be which cerebral artery supplies blood flow. When regions were grouped according to cerebral artery supply, we noted higher microvascular loss in regions supplied by the ACA than the MCA or PCA. It is possible that the ACA may have less redundancy or collateral flow than branches of the MCA and PCA. Indeed, a study using time resolved computed tomography angiography revealed weaker collateral connections between the MCA and ACA, and stronger ones connecting MCA with PCA.[35] With reduced collateral circulation, regions supplied by the ACA may have less resilience to interruptions or changes in blood flow that can occur throughout life.[43] Alternatively, the PCA does not appear to experience as large of an age-related drop in blood flow rates as the ACA or MCA,[44] which could conceivably change capillary plugging or recanalization rates in a region-dependent manner. While speculative, an ACA-specific susceptibility to microvascular loss also would fit with the frontal lobe theory of aging,[45–47] where reduced nutrient delivery due to low microvascular density could contribute to frontal dysfunction.

Even though our data agree with past studies examining vessel loss in cortex and hippocampus, the magnitude of loss tended to be lower in our study (Supplementary Table 2). The reason for this difference could be methodological in nature. The majority of previous studies used enzyme or immunohistochemical approaches to label the vasculature. It is possible that the expression of these vascular proteins could be affected by age and thus influence measurements. We opted to avoid this potential issue by injecting a fluorescent dye in vivo to label all perfused vessels and then collected the brain without intracardial perfusion. This approach was also compatible with our experiment assessing the regional distribution of fluorescent microspheres, which would have been disrupted if we employed a standard transcardial perfusion approach for immunohistochemistry. It is important to note that our method for labeling and quantifying vascular length yielded results (typically $\sim 1\ m/mm^3$ for sensory cortical areas) that closely match more recent estimates.[4,39,48,49]

Based on our previous work in the somatosensory cortex, we know that capillaries with long-lasting obstructions are pruned in ~30% of cases.[24] In order to better understand why certain brain regions were more vulnerable to vessel loss with aging than others, we hypothesized that those regions prone to long-lasting obstructions, ones evident 3 days after induction, would show greater vessel loss. Indeed, our data support this idea given that brain regions with higher

Figure 6. Continued.
local rupture of the blood brain barrier. As a positive control (right), we show microglia aggregation around a cortical capillary ruptured in vivo. Scale bar = 20 μm. (d) Graphs show the density of short (30 min) or long-lived (3 days) microsphere obstructions across each brain region in young adult and aged mice (30 min: $F_{(4.035,60.52)} = 19.54$, $p < 0.0001$ and 3 days: $F_{(4.235,59.29)} = 3.7.890$, $p < 0.0001$). (e) Graphs plot the % clearance of obstructions (1–3 day/30 min density) to illustrate significant variability across brain regions ($F_{(4.265,59.71)} = 3.840$, $p = 0.0066$). (f) Regression analysis of short or long-lived obstruction density (30 min vs. 3 days) for each brain region plotted as a function of vessel loss with aging. With the exception of the retrosplenial (RS) cortex, which was a clear outlier at both time points (identified by Grubbs test), the density of long-lived obstructions (3 days) in each brain region was significantly related to the extent of vessel loss with aging. (g) Similarly, regression analysis indicated that those brain regions more adept at clearing obstructions (higher % clearance rate values), were less likely to show age-related vessel loss. Note that these relationships were stronger for white and cortical grey matter (middle panel in (f) and (g)) than for subcortical grey matter (right panel in (f) and (g)). Data presented in (d) and (e) were analyzed using one-way repeated measures ANOVA.

rates of microsphere induced obstructions (and lower microsphere clearance rates) were also more likely to show greater vessel loss. However, this is an admittedly simplistic explanation of vessel loss since it is possible that vessel loss may be compensated for by angiogenesis.[14] While previous time lapse imaging experiments in somatosensory cortex, both from our lab and from others, report little and sometimes no compensatory vessel sprouting in healthy adult animals,[24,50–54] other regions, particularly subcortical regions that did not show significant vessel loss, may balance capillary rarefaction with angiogenesis. Our study is also limited by the fact that we did not test regional differences in susceptibility to naturally occurring obstructions such as blood cells or lipids. However, given how infrequent these naturally occurring events are (more persistent natural obstructions affect $<1\%$ of all capillaries), as well the impossibility of estimating the duration of capillary obstruction without time lapse *in vivo* imaging in all 15 regions, we opted to study capillary plugging rates with microspheres. We should note that capillary pruning rates for long-lasting microsphere induced obstructions are nearly identical to those that occur naturally.[24] Our study also did not examine regional differences in how capillaries clear obstructions. For example, engulfing and removing obstructions through the vessel wall (angiophagy) is a process that requires several days as opposed to embolus washout.[55–57] It is conceivable that angiophagy may show regional differences which could explain why retrosplenial cortex exhibited unusually high obstruction rates at 30 min and 3 days yet showed relatively normal vessel loss with aging. Future studies employing time lapse imaging in multiple regions, especially in deep tissues, would be helpful in resolving these issues.

The functional significance of age and brain region-specific vessel loss remains an important question. Cognitive testing in humans and experimental animals has revealed that some functions, such as working memory, attention, speed of information processing and sensory-motor function are particularly vulnerable to aging.[58] Given the central role of the limbic cortex, hippocampus, corpus callosum and somatosensory-motor cortex in these functions, it is conceivable that progressive loss of microvascular structure in these regions may underlie some of these changes. Indeed, several studies show that microvascular pathology precedes or at least accompanies cognitive impairments that occur with aging or neurodegenerative disease.[8,59–62] While the reasons for region specific vulnerabilities to vessel loss remain speculative, our findings suggest that susceptibility to capillary obstructions and/or inability to clear these obstructions represents at least one plausible factor. We anticipate our study will provide key normative data for future studies, especially in brain regions not well characterized (e.g. retrosplenial, peri-rhinal cortex, substantia nigra), to interpret vessel loss in premature aging or neuropathological conditions.

Funding

The author(s) declared the following potential conflicts of interest with respect to the research, authorship, and/or publication of this article: This work was supported by operating, salary and equipment grants to CEB from the Canadian Institutes of Health Research (CIHR), Heart and Stroke Foundation (HSF), Natural Sciences and Engineering Research Council of Canada (NSERC), Canadian Foundation for Innovation (CFI). BS was supported by a graduate fellowship from CIHR.

Acknowledgements

The authors would like to thank Taimei Yang for managing our mouse colony, Alexis Kellinghusen for assistance with data collection and Dr. Patrick Reeson for his important insights in the initial studies.

Declaration of conflicting interests

The author(s) declared no potential conflicts of interest with respect to the research, authorship, and/or publication of this article.

Authors' contributions

BS and CEB conceived the study and wrote the manuscript. BS performed experiments and analyzed data.

Supplementary material

Supplemental material for this article is available online.

References

1. Attwell D and Laughlin SB. An energy budget for signaling in the grey matter of the brain. *J Cereb Blood Flow Metab* 2001; 21: 1133–1145.
2. Peters A, Schweiger U, Pellerin L, et al. The selfish brain: competition for energy resources. *Neurosci Biobehav Rev* 2004; 28: 143–180.
3. Zhang S, Boyd J, Delaney K, et al. Rapid reversible changes in dendritic spine structure in vivo gated by the degree of ischemia. *J Neurosci* 2005; 25: 5333–5338.
4. Tsai PS, Kaufhold JP, Blinder P, et al. Correlations of neuronal and microvascular densities in murine cortex revealed by direct counting and colocalization of nuclei and vessels. *J Neurosci* 2009; 29: 14553–14570.
5. Blinder P, Tsai PS, Kaufhold JP, et al. The cortical angiome: an interconnected vascular network with noncolumnar patterns of blood flow. *Nat Neurosci* 2013; 16: 889–897.
6. Gould IG, Tsai P, Kleinfeld D, et al. The capillary bed offers the largest hemodynamic resistance to the cortical blood supply. *J Cereb Blood Flow Metab* 2017; 37: 52–68.

7. Ruitenberg A, den Heijer T, Bakker SLM, et al. Cerebral hypoperfusion and clinical onset of dementia: the Rotterdam study. *Ann Neurol* 2005; 57: 789–794.
8. Iadecola C. The pathobiology of vascular dementia. *Neuron* 2013; 80: 844–866.
9. Østergaard L, Jespersen SN, Engedahl T, et al. Capillary dysfunction: its detection and causative role in dementias and stroke. *Curr Neurol Neurosci Rep* 2015; 15: 37.
10. Joo IL, Lai AY, Bazzigaluppi P, et al. Early neurovascular dysfunction in a transgenic rat model of Alzheimer's disease. *Sci Rep* 2017; 7: 46427.
11. Nielsen RB, Egefjord L, Angleys H, et al. Capillary dysfunction is associated with symptom severity and neurodegeneration in Alzheimer's disease. *Alzheimers Dement* 2017; 13: 1143–1153.
12. Cruz-Hernández JC, Bracko O, Kersbergen CJ, et al. Neutrophil adhesion in brain capillaries reduces cortical blood flow and impairs memory function in Alzheimer's disease mouse models. *Nat Neurosci* 2019; 22: 413.
13. Riddle DR, Sonntag WE and Lichtenwalner RJ. Microvascular plasticity in aging. *Ageing Res Rev* 2003; 2: 149–168.
14. Ndubuizu OI, Tsipis CP, Li A, et al. Hypoxia inducible factor-1 (HIF-1) independent microvascular angiogenesis in the aged rat brain. *Brain Res* 2010; 1366: 101–109.
15. Brown WR and Thore CR. Review: cerebral microvascular pathology in ageing and neurodegeneration. *Neuropathol Appl Neurobiol* 2011; 37: 56–74.
16. Xu X, Wang B, Ren C, et al. Age-related impairment of vascular structure and functions. *Aging Dis* 2017; 8: 590–610.
17. Gunning-Dixon FM and Raz N. The cognitive correlates of white matter abnormalities in normal aging: a quantitative review. *Neuropsychology* 2000; 14: 224–232.
18. Raz N, Lindenberger U, Rodrigue KM, et al. Regional brain changes in aging healthy adults: general trends, individual differences and modifiers. *Cereb Cortex* 2005; 15: 1676–1689.
19. Alexander GE, Ryan L, Bowers D, et al. Characterizing cognitive aging in humans with links to animal models. *Front Aging Neurosci* 2012; 4: 21.
20. Badhwar A, Brown R, Stanimirovic DB, et al. Proteomic differences in brain vessels of Alzheimer's disease mice: normalization by PPARγ agonist pioglitazone. *J Cereb Blood Flow Metab* 2017; 37: 1120–1136.
21. Mattson MP and Arumugam TV. Hallmarks of brain aging: adaptive and pathological modification by metabolic states. *Cell Metab* 2018; 27: 1176–1199.
22. Santisakultarm TP, Paduano CQ, Stokol T, et al. Stalled cerebral capillary blood flow in mouse models of essential thrombocythemia and polycythemia vera revealed by in vivo two-photon imaging. *J Thromb Haemost JTH* 2014; 12: 2120–2130.
23. Erdener ŞE, Tang J, Sajjadi A, et al. Spatio-temporal dynamics of cerebral capillary segments with stalling red blood cells. *J Cereb Blood Flow Metab* 2017; 39: 886–900.
24. Reeson P, Choi K and Brown CE. VEGF signaling regulates the fate of obstructed capillaries in mouse cortex. *eLife* 2018; 7: e33670.
25. Forde A, Constien R, Gröne H-J, et al. Temporal Cre-mediated recombination exclusively in endothelial cells using Tie2 regulatory elements. *Genesis* 2002; 33: 191–197.
26. Hooper AT, Butler JM, Nolan DJ, et al. Engraftment and reconstitution of hematopoiesis is dependent on VEGFR2-mediated regeneration of sinusoidal endothelial cells. *Cell Stem Cell* 2009; 4: 263–274.
27. Arganda-Carreras I, Kaynig V, Rueden C, et al. Trainable Weka Segmentation: a machine learning tool for microscopy pixel classification. *Bioinformatics* 2017; 33: 2424–2426.
28. Franklin K and Paxinos G. *The mouse brain in stereotaxic coordinates*. 3rd ed. New York: Academic Press, 2008.
29. Schager B. Microvessel density analysis. GitHub, https://github.com/bschager/Microvessel-Density-Analysis (2019, accessed 2 August 2019).
30. Bagi Z, Brandner DD, Le P, et al. Vasodilator dysfunction and oligodendrocyte dysmaturation in aging white matter. *Ann Neurol* 2018; 83: 142–152.
31. Bennett IJ and Madden DJ. Disconnected aging: cerebral white matter integrity and age-related differences in cognition. *Neuroscience* 2014; 276: 187–205.
32. Birdsill AC, Koscik RL, Jonaitis EM, et al. Regional white matter hyperintensities: aging, Alzheimer's disease risk, and cognitive function. *Neurobiol Aging* 2014; 35: 769–776.
33. de Groot M, Ikram MA, Akoudad S, et al. Tract-specific white matter degeneration in aging: the Rotterdam study. *Alzheimers Dement* 2015; 11: 321–330.
34. Ng YS, Stein J, Ning M, et al. Comparison of clinical characteristics and functional outcomes of ischemic stroke in different vascular territories. *Stroke* 2007; 38: 2309–2314.
35. Menon BK, O'Brien B, Bivard A, et al. Assessment of leptomeningeal collaterals using dynamic CT angiography in patients with acute ischemic stroke. *J Cereb Blood Flow Metab* 2013; 33: 365–371.
36. Moeini M, Lu X, Avti PK, et al. Compromised microvascular oxygen delivery increases brain tissue vulnerability with age. *Sci Rep* 2018; 8: 8219.
37. Amenta F, Ferrante F, Mancini M, et al. Effect of long-term treatment with the dihydropyridine-type calcium channel blocker darodipine (PY 108-068) on the cerebral capillary network in aged rats. *Mech Ageing Dev* 1995; 78: 27–37.
38. Amenta F, Cavallotti D, Del Valle M, et al. Age-related changes in brain microanatomy: sensitivity to treatment with the dihydropyridine calcium channel blocker darodipine (PY 108-068). *Brain Res Bull* 1995; 36: 453–460.
39. Murugesan N, Demarest TG, Madri JA, et al. Brain regional angiogenic potential at the neurovascular unit during normal aging. *Neurobiol Aging* 2012; 33: 1004.e1–1004.e16.
40. Villena A, Vidal L, Díaz F, et al. Stereological changes in the capillary network of the aging dorsal lateral geniculate nucleus. *Anat Rec A Discov Mol Cell Evol Biol* 2003; 274A: 857–861.

41. Tong X-K, Trigiani LJ and Hamel E. High cholesterol triggers white matter alterations and cognitive deficits in a mouse model of cerebrovascular disease: benefits of simvastatin. *Cell Death Dis* 2019; 10: 89.
42. Li B, Ohtomo R, Thunemann M, et al. Two-photon microscopic imaging of capillary red blood cell flux in mouse brain reveals vulnerability of cerebral white matter to hypoperfusion. *J Cereb Blood Flow Metab*. Epub ahead of print 4 March 2019. DOI: 10.1177/0271678X19831016.
43. Ma J, Ma Y, Shuaib A, et al. Impaired collateral flow in pial arterioles of aged rats during ischemic stroke. *Transl Stroke Res*. Epub ahead of print 15 June 2019. DOI: 10.1007/s12975-019-00710-1.
44. Zarrinkoob L, Ambarki K, Wåhlin A, et al. Blood flow distribution in cerebral arteries. *J Cereb Blood Flow Metab* 2015; 35: 648–654.
45. Greenwood PM. The frontal aging hypothesis evaluated. *J Int Neuropsychol Soc JINS* 2000; 6: 705–726.
46. Pugh KG and Lipsitz LA. The microvascular frontal-subcortical syndrome of aging. *Neurobiol Aging* 2002; 23: 421–431.
47. Nyberg L, Salami A, Andersson M, et al. Longitudinal evidence for diminished frontal cortex function in aging. *Proc Natl Acad Sci* 2010; 107: 22682–22686.
48. Lugo-Hernandez E, Squire A, Hagemann N, et al. 3D visualization and quantification of microvessels in the whole ischemic mouse brain using solvent-based clearing and light sheet microscopy. *J Cereb Blood Flow Metab* 2017; 37: 3355–3367.
49. Xiong B, Peng J, Li A, et al. Precise cerebral vascular Atlas in stereotaxic coordinates of whole mouse brain. *Front Neuroanat* 2017; 11: 128.
50. Mostany R, Chowdhury TG, Johnston DG, et al. Local hemodynamics dictate long-term dendritic plasticity in peri-infarct cortex. *J Neurosci* 2010; 30: 14116–14126.
51. Harb R, Whiteus C, Freitas C, et al. In vivo imaging of cerebral microvascular plasticity from birth to death. *J Cereb Blood Flow Metab Off J Int Soc Cereb Blood Flow Metab* 2013; 33: 146–156.
52. Tennant KA and Brown CE. Diabetes augments in vivo microvascular blood flow dynamics after stroke. *J Neurosci* 2013; 33: 19194–19204.
53. Masamoto K, Takuwa H, Seki C, et al. Microvascular sprouting, extension, and creation of new capillary connections with adaptation of the neighboring astrocytes in adult mouse cortex under chronic hypoxia. *J Cereb Blood Flow Metab* 2014; 34: 325–331.
54. Cudmore RH, Dougherty SE and Linden DJ. Cerebral vascular structure in the motor cortex of adult mice is stable and is not altered by voluntary exercise. *J Cereb Blood Flow Metab* 2017; 37: 3725–3743.
55. Lam CK, Yoo T, Hiner B, et al. Embolus extravasation is an alternative mechanism for cerebral microvascular recanalization. *Nature* 2010; 465: 478–482.
56. Grutzendler J, Murikinati S, Hiner B, et al. Angiophagy prevents early embolus washout but recanalizes microvessels through embolus extravasation. *Sci Transl Med* 2014; 6: 226ra31–226ra31.
57. van der Wijk A-E, Lachkar N, de Vos J, et al. Extravasation of microspheres in a rat model of silent brain infarcts. *Stroke* 2019; 50: 1590–1594.
58. Murman DL. The impact of age on cognition. *Semin Hear* 2015; 36: 111–121.
59. Bell RD and Zlokovic BV. Neurovascular mechanisms and blood-brain barrier disorder in Alzheimer's disease. *Acta Neuropathol (Berl)* 2009; 118: 103–113.
60. Brown WR, Moody DM, Thore CR, et al. Microvascular changes in the white mater in dementia. *J Neurol Sci* 2009; 283: 28–31.
61. Iturria-Medina Y, Sotero RC, Toussaint PJ, et al. Early role of vascular dysregulation on late-onset Alzheimer's disease based on multifactorial data-driven analysis. *Nat Commun* 2016; 7: 11934.
62. Østergaard L, Engedal TS, Moreton F, et al. Cerebral small vessel disease: capillary pathways to stroke and cognitive decline. *J Cereb Blood Flow Metab* 2016; 36: 302–325.